Performance Comparison of Available Interstitial Antennas for Microwave Hyperthermia

AMER M. TUMEH AND MAGDY F. ISKANDER, SENIOR MEMBER, IEEE

Abstract—The use of interstitial antennas for microwave hyperthermia has gained popularity because of the increased utilization of invasive treatment techniques using radioactive seeds. This method of directly applying therapeutic heating has the advantage of causing minimal damage to the surrounding healthy tissue and it helps achieve heating of deep-seated tumors. Several designs of interstitial antennas are commercially available and there is a need to evaluate and compare their performance. In a recent paper [1], an experimental comparison was made between three different antennas: the Dartmouth, the BSD Medical, and the Cheung. Many of the commercially available antenna designs are multisections, while available analytical techniques are only valid for uniformly insulated antennas.

We have developed a numerical model which calculates the current distribution and radiation characteristics of multisection antennas having varying diameters of the center conductor and/or the types and thicknesses of the insulation. In this paper we briefly describe the model and compare the numerical results with the experimental data published by Ryan and Strohbehn [1]. Excellent correlation between the experimental and calculated patterns was obtained. The numerical model was then used to examine some interesting changes in the commercial designs, such as the effect of the tip termination of the antenna and the diameters of the conducting sections (collars) on the heating patterns of the BSD Medical antenna. Important observations regarding the role of each section, in multisection antenna designs, in guiding along the antenna versus coupling to the ambient were also investigated and verified.

I. INTRODUCTION

ONE OF THE MAIN objectives of using microwaves in hyperthermia for cancer treatment is to develop the capability of delivering therapeutic heat to deep-seated tumors without overheating the surrounding healthy tissue. Among the large varieties of antennas that may be used in this application, including waveguide applicators, phased-array applicators, and other applicators of the capacitive and inductive type, the use of interstitial antennas has recently seen a dramatic increase. This is because these antennas provide several advantages, including direct heating of tumors with minimum damage to surrounding tissue, simplicity of controlling the heating pattern using arrays, and the possibility of simultaneously measuring the temperature distribution using thermistors attached to the antenna. The popularity of interstitial antennas has been further extended because of the increased clinical employment of invasive treatment techniques using ionizing radiation.

Over the past two years we have designed and optimized the performance of multisection insulated antennas for hyperthermia treatment [2]–[4]. To improve the design performance of interstitial antennas, parameters such as the uniformity of heating pattern, the depth of penetration, and the impedance-matching properties were optimized. Therefore, the optimization procedure requires identifying and quantifying the trade-offs between various design parameters, including the diameters of the center conductor and the insulation, the type of insulation, and the feasibility of using multisection antennas to achieve the desired optimum designs. The multisection insulated antennas were evaluated numerically by calculating their current distribution and the irradiation characteristics in conductive media. The numerical predictions were verified experimentally both by making heating pattern measurements and by mapping the various near- and far-field components of these antennas [2]–[4].

Several designs of interstitial antennas are commercially available and there is a need to evaluate and compare their performance. Recently, an experimental comparison was made between three different antennas: the Dartmouth, the BSD Medical, and the Cheung [1]. Although many of the antenna designs are multisection, previously available analytical techniques are limited to uniformly insulated antennas [5].

In this paper we compare the numerical results obtained using our new numerical model [2]–[4] with the experimental data published by Ryan and Strohbehn [1]. Specific comparisons between the published experimental heating patterns and those predicted by our model are discussed. Based on this comparison, the advantages of the developed numerical model and its value in making it possible to make a fairly accurate preliminary judgment regarding the resulting heating pattern based on the α/β radiation coupling factor are emphasized.

Manuscript received April 7, 1988, revised February 21, 1989.

A. M. Tumeh was with the Electrical Engineering Department, University of Utah, Salt Lake City, UT 84112. He is now with the BSD Medical Corporation, Salt Lake City, UT.

M. F. Iskander is with the Electrical Engineering Department, University of Utah, Salt Lake City, UT 84112.

IEEE Log Number 8927789.

0018-9480/89/0700-1126$01.00

II. Numerical Model

Previously, we developed and reported [2], [3] the theory of multisection insulated antennas in conductive media. The theory is based on generalizing the rigorous solution developed by King *et al.* [5] for uniformly insulated antennas, and extending it to the case of multisection antennas. One of the most important conclusions derived from the extensive analysis conducted by King on insulated antennas [6] is that such antennas, when placed in dissipative media, may be treated as sections of lossy transmission lines with generalized propagation constants that account for the ohmic losses in the conductors as well as for the losses due to radiation from the antenna to the ambient medium. Therefore, a possible procedure for analyzing a multisection insulated antenna in a dissipative medium is through the representation of the antenna by a multisection transmission line, where each section is terminated with a load impedance equal to the input impedance of the preceding section. Hence, for the ith section of the antenna, the input impedance and the current distribution are given by

$$Z_{\text{in}}^{i} = jZ_c^i/\tan\left[K_{Li}h_i + j\theta_{hi}\right] \tag{1}$$

$$I_{zi}(z) = Y_{\text{in}}^{i}(z)\frac{\sin\left[K_{Li}(h_i - |z|) + j\theta_{hi}\right]}{\sin\left(K_{Li}h_i + j\theta_{hi}\right)} \tag{2}$$

where $\theta_{hi} = \coth^{-1}[Z_{\text{in}}^{(i-1)}/Z_c^i]$ is the angle used to take into account the termination of the ith section of the antenna with the load impedance $Z_{\text{in}}^{(i-1)}$, which is the input impedance of the $(i-1)$th section of the antenna. The parameters h_i, Z_c^i, and K_{Li} are the length, characteristic impedance, and propagation constant, respectively, of the ith section. The propagation constant, K_{Li}, and the characteristic impedance, Z_c^i, are given elsewhere [5]. These parameters basically depend on the diameters of the conductors and the insulation in each section, the complex permittivity of the ambient, and the type of insulation used as a catheter [5], [6].

The above procedure is used to calculate the input impedance and the current distribution of multisection antennas. To calculate the radiated fields from a multisection insulated antenna, we divide the antenna into an array of point-source (infinitesimal electric dipoles) distributions along the insulation. The magnitude and phase distribution among these point sources are determined by [2]:

1) The magnitude and phase of the current distribution along the antenna as given in (2).
2) The magnitude of the point sources is further multiplied by what we call the radiation efficiency term, which is equal to α/β, where α and β are the real and imaginary parts of the complex propagation constant $K_L = \alpha + j\beta$. It should be noted that this radiation efficiency term α/β is proportional to the radiation losses to the ambient medium per wavelength. The inclusion of this intensity-modifying factor was found to be particularly important for accurately calculating the power deposition pattern in the near zone of the interstitial antennas.
3) In calculating the radiation characteristics of interstitial antennas, we add the vector fields obtained from the near-field radiation from a large number of point sources distributed along the antenna. The fields from each point source are given by

$$E_r(r,\theta) = \frac{J_e(z_m)}{2\pi}e^{-jK_4 r}\left(\frac{\eta}{r^2} + \frac{1}{j\omega\epsilon_4^* r^3}\right)\cos\theta \tag{3}$$

$$E_\theta(r,\theta) = \frac{J_e(z_m)}{4\pi} \cdot e^{-jK_4 r}\left(\frac{j\omega\mu_0}{r} + \frac{\eta}{r^2} + \frac{1}{j\omega\epsilon_4^* r_3}\right)\sin\theta \tag{4}$$

where the amplitude (magnitude and phase) of the mth point source (infinitesimal electric dipole), $J_e(z_m)$, located at z_m along the antenna, is given by

$$J_e(z_m) = (\alpha_m/\beta_m)I_z(z_m) \tag{5}$$

where $I_z(z_m)$ is the amplitude of the current from (2) at the location of the point source z_m. In (3) and (4), K_4 is the propagation constant in the ambient medium, η is the intrinsic impedance of the ambient medium $\eta = \sqrt{\mu_0/\epsilon_4^*}$, r is the distance between a point source and the observation point, and ϵ_4^* is the complex permittivity of the surrounding medium.

It should be noted that the proposed numerical model is different from that utilized by Turner [8]. While in [8] the point-source distribution model was utilized, no attempt was made to model the intensity of these point sources according to the realistic current distribution in the multisection antenna described here. Furthermore, in our model we introduced the radiation efficiency factor (α/β), which accounts for the radiation losses to the ambient medium based on the propagation constant in each of the insulated sections of the antenna.

This numerical model was used to optimize the performance of interstitial antennas [2]–[4]. Since then, however, experimental data comparing the performance of three commercially available antennas have been published [1]. In this paper we calculate the heating patterns of these commercially available antennas using the developed numerical model and compare the results obtained with the published experimental data.

III. Results

As indicated earlier in this paper, we compare the results of the developed numerical model for three commercially available interstitial antennas with the recently published experimental data. The antennas studied are the Dartmouth D9, the BSD Medical, and the Cheung [1], [7]–[9]. The Dartmouth D9 antenna consists of an enlarged extension of the center conductor of a coaxial transmission line with a 1 mm junction between the dipole portions. The antenna is 4 cm long and has a 1 mm outer diameter. The BSD antenna is a more complex design

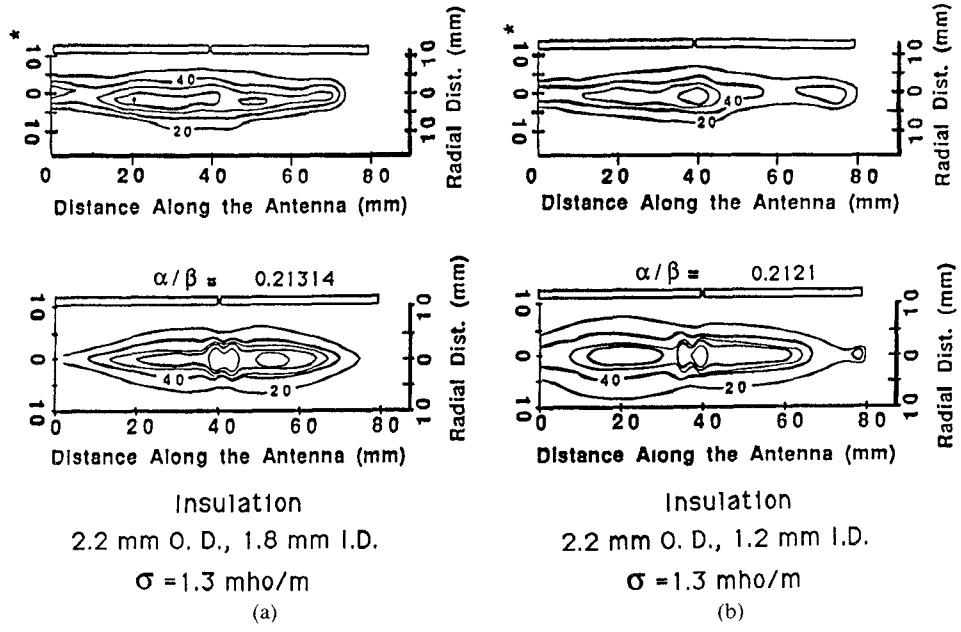

Fig. 1 Comparison between the numerical (bottom) and experimental (top) results of the power deposition pattern of the Dartmouth D9 interstitial antenna. The patterns were calculated in a muscle-equivalent phantom of conductivity $\sigma = 1.3$ mho/m and dielectric constant $\epsilon_r = 50$ at 915 MHz. Two catheter sizes were used: (a) 2.2 mm OD and 1.8 mm ID, and (b) 2.2 mm OD and 1.2 mm ID (* Ryan and Strohbehn [1]).

which consists of multisections of different lengths and diameters. The total antenna length is 4.5 cm and the outer diameters range from 0.2 to 1.07 mm [8]. The Cheung Hot-Tip antenna consists of two sections with different diameters, extending from the center conductor of a coaxial transmission line [9]. The Cheung antenna is 1.5 cm long and has an outer diameter of 0.8 mm for the longer section.

The numerical calculations of the heating patterns of these antennas are presented in two segments. First, we calculated the power deposition patterns using the same parameters as those used by Ryan and Strohbehn [1]. We also altered some of the design parameters and examined the sensitivity of the heating patterns to these variations. The power deposition patterns of these antennas were calculated and compared with the experimental results for two cases: in catheters of 2.2 mm OD and 1.2 mm ID and when placed in 2.2 mm OD and 1.8 mm ID catheters. As in the experimental data, a muscle-equivalent phantom material with a conductivity of 1.3 mho/m and a dielectric constant of 50 at 915 MHz is assumed to be the lossy medium surrounding the insulated antennas.

Fig. 1 shows the measured and calculated heating patterns of the Dartmouth antenna for the two different catheter sizes. The numerical results are in excellent agreement with the experimental data published by Ryan and Strohbehn [1]. The main feature of the power deposition pattern of this antenna is that most of the energy is deposited in the region near the feed point of the antenna, with some increased heating at the tip for the case of the thicker catheter wall. Fig. 2 shows the heating patterns of the Cheung Hot-Tip antenna placed in the same two catheters given in Fig. 1. since the antenna consists of two sections with different diameters, the ratio of the diameter of the insulation to that of the center conductor is larger for the section close to the feed than for the section away from the feed. Therefore, the thicker insulation of the section close to the feed helps in guiding the EM energy through the antenna, and the thinner insulation of the second section near the tip helps in the efficient coupling of the EM energy to the ambient conductive medium. By comparing the value of the radiation efficiency term of Fig. 2(b) in the feed section, $\alpha/\beta = 0.176$, to that of the tip section, $\alpha/\beta = 0.209$, it is clear that with the thinner insulation at the tip, the losses per wavelength α/β are larger. This is clearly reflected in the power deposition patterns shown in Fig. 2, which shows a greater concentration of the power deposited at the tip of the antenna. Comparing this power deposition pattern to that of Ryan and Strohbehn [1], we notice that our model predicts power concentrations at the antenna tip as well as around the feed region, and a lower power deposition about 0.5 cm from the tip of the antenna. The main features of the reported experimental data have thus been confirmed using the numerical model.

Fig. 3 shows the power deposition patterns for the BSD antenna. The insulation thickness is 2.2 mm OD and 1.8 mm ID for the first catheter and 2.2. mm OD and 1.2 mm ID for the second. The values of radiation efficiency terms α/β (e.g., 0.217, 0.203, 0.139, 0.203, 0.217 for case (b)) in the various sections are also given in Fig. 3. Examining the values of α/β of those sections shows that α/β is maximum in the two enlarged collars which have the thinnest insulation of all the sections, and α/β is minimum in the middle section, which has the thickest insulation. Therefore, the two collar sections have more

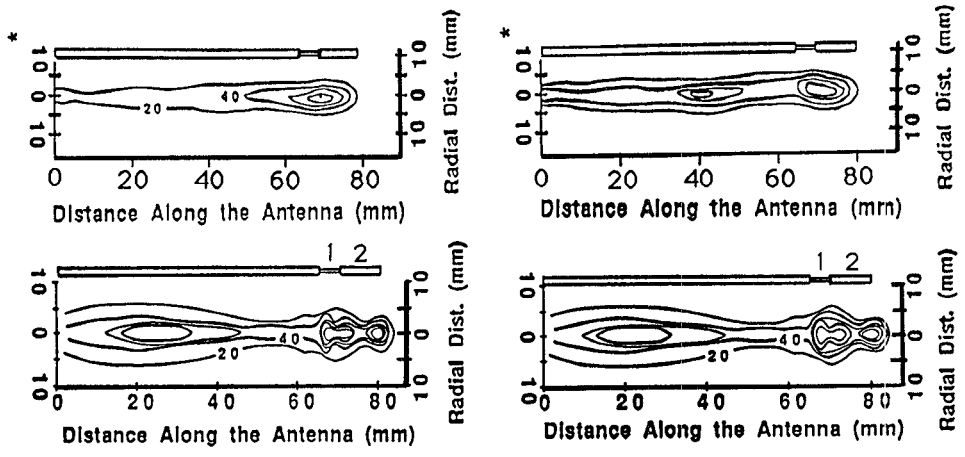

Section No.	1	2
α / β	0.174	0.206

(a)

Section No.	1	2
α / β	0.176	0.209

(b)

Fig. 2. Comparison between the numerical (bottom) and experimental (top) results of the power deposition pattern of the Cheung Hot-Tip interstitial antenna. The patterns were calculated in a muscle-equivalent phantom of conductivity σ = 1.3 mho/m and dielectric constant ϵ_r = 50 at 915 MHz. Two catheter sizes were used: (a) 2.2 mm OD and 1.8 mm ID, and (b) 2.2 mm OD and 1.2 mm ID (* Ryan and Strohbehn [1]).

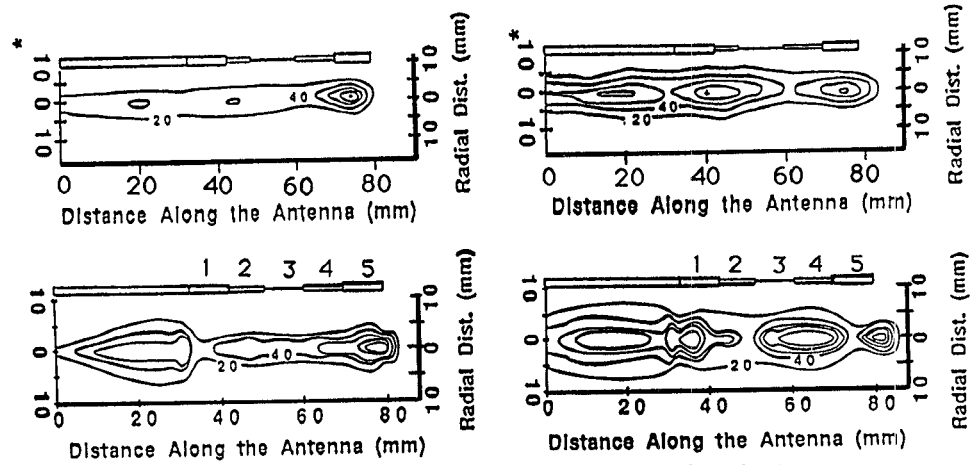

Section No.	1	2	3	4	5
α / β	0.218	0.210	0.139	0.203	0.218

(a)

Section No.	1	2	3	4	5
α / β	0.217	0.203	0.139	0.203	0.217

(b)

Fig. 3. Comparison between the numerical (bottom) and experimental (top) results of the power deposition pattern of the BSD Medical interstitial antenna. The patterns were calculated in a muscle-equivalent phantom of conductivity σ = 1.3 mho/m and dielectric constant ϵ_r = 50 at 915 MHz. Two catheter sizes were used: (a) 2.2 mm OD and 1.8 mm ID, and (b) 2.2 mm OD and 1.2 mm ID (* Ryan and Strohbehn [1]).

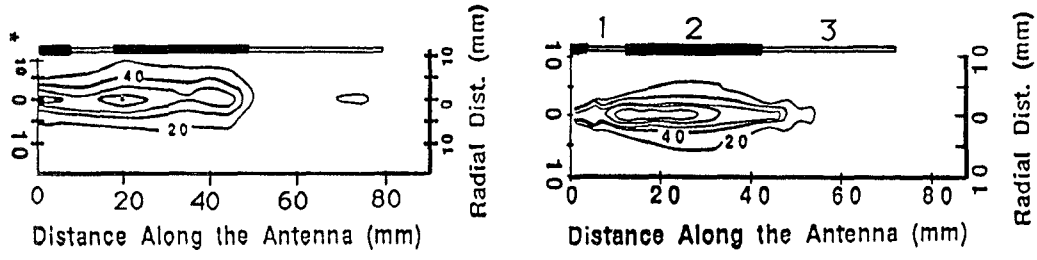

Insulation
2.2 mm O. D., 1.2 mm I.D.
σ = 1.3 mho/m

(a)

Insulation
2.2 mm O. D., 1.2 mm I.D.
σ = 1.3 mho/m

Section No.	1	2	3
α/β	0.139	0.209	0.139

(b)

Fig. 4. Comparison between the numerical (b) and experimental (a) results of the power deposition pattern of the Cheung two-node interstitial antenna. The patterns were calculated in a muscle-equivalent phantom of conductivity $\sigma = 1.3$ mho/m and dielectric constant $\epsilon_r = 50$ at 915 MHz. Two catheter sizes were used: (a) 2.2 mm OD and 1.8 mm ID, and (b) 2.2. mm OD and 1.2 mm ID (* Ryan and Strohbehn [1]).

coupling efficiency to the ambient medium than the middle section, which acts as a guiding section for the EM energy to the antenna tip. The power deposition pattern of Fig. 3(a) illustrates the tip heating of the BSD antenna, where the dimensions of the insulating catheter have played a key role in obtaining such a pattern. The smaller catheter wall thickness of Fig. 3(a) (compared with the second insulating catheter of Fig. 3(b)) results in a wider air gap between the antenna and the insulation, thus allowing more energy to be guided to the antenna tip. The power deposition pattern of Fig. 3(b) shows concentrations of energy around the feed, the tip, and the middle section of the antenna. Notice that the intensity of the power deposited at the tip of the antenna is similar to the power intensities at the middle section and at the collar section close to the feed. By comparing the calculated power patterns of Fig. 3 to that of the experimental data, we notice that there is good agreement between the two patterns, where the trends are basically the same in both the numerical and the experimental results.

Fig. 4 shows the power deposition pattern of the Cheung two-node antenna when placed in a 2.2 mm OD and 1.2 mm ID catheter. The radiation efficiency terms α/β (0.139, 0.209, 0.139) are also given in Fig. 4(b). Comparison of the power patterns of Fig. 4 with that of the experimental data shows very good correlation between the two patterns, where the EM energy was guided through the feed section and radiated through the middle section. Notice that the radiation efficiency term is the largest in the middle section of the antenna, and that is where most of the energy was radiated to the ambient medium. Since most of the radiation took place in the middle section and practically no power was left to be radiated from the tip section, the radiation from the end section of the antenna becomes immaterial, which is the case in Fig. 4.

From the given results it is clear that there is an excellent correlation between the numerical and the experimental data. The numerical model and, specifically, parameters such as the radiation efficiency factor, α/β, provide insight into the behavior of the obtained power deposition patterns and the radiation versus the guiding roles of the various sections in the multisection antenna designs. For example, it is interesting to compare the Hot-Tip with the two-node Cheung design (Figs. 2 and 4, respectively). In the Hot-Tip design of Fig. 2, the radiation efficiency term, α/β, of the first section near the feed was sufficiently small so that this section played the role of guiding the electromagnetic energy to the end section rather than radiating it. It is this effective guiding property, as well as the higher radiation efficiency, $\alpha/\beta = 0.209$, at the end section of Fig. 2(b), that resulted in a "hot tip" in the power deposition pattern. In the two-node design, on the other hand, the middle section has the maximum radiation efficiency factor ($\alpha/\beta = 0.209$). Therefore, the first section played the role of guiding the energy, and the middle section coupled (including radiation) the electromagnetic energy to the surrounding ambient medium. The length of the middle section was chosen to be sufficiently long so that most of the energy was coupled along its length. This leaves no energy to the third (top) section to couple to the ambient medium, and such an observation is clearly confirmed in Fig. 4. Therefore, we conclude that for the specific design shown in Fig. 4 [1], there is effectively no need for the last (top) section of the antenna. If the middle section had been made shorter or the diameter of the conductor decreased, on the other hand, some of the

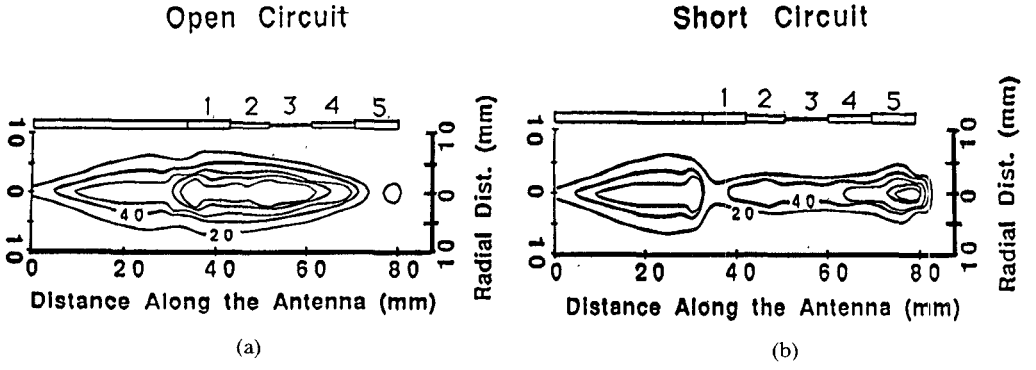

Section No.	1	2	3	4	5
α/β	0.218	0.210	0.139	0.203	0.218

Insulation
2.2 mm O. D., 1.8 mm I.D.
σ =3.0 mho/m

Fig. 5 Comparison between the power deposition pattern of the BSD Medical interstitial antenna for two different tip terminations: (a) open-circuit tip, and (b) short-circuit tip, whereby the center conductor is connected to the outer conductor of the coaxial antenna. The short-circuit tip is the one used in the design of the BSD Medical antenna. The power patterns were calculated in a muscle-equivalent phantom of conductivity $\sigma = 1.3$ mho/m and dielectric constant $\epsilon_r = 50$ at 915 MHz.

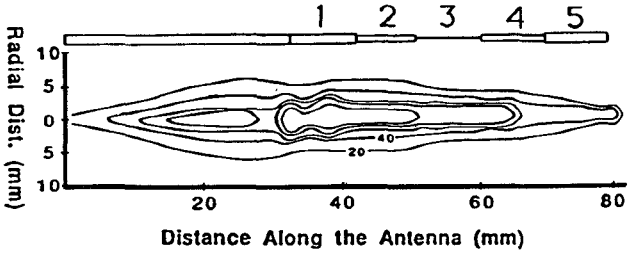

Section No.	1	2	3	4	5
α/β	0.205	0.195	0.122	0.187	0.205

Insulation
2.2 mm O. D., 1.2 mm I.D.
σ =3.0 mho/m

Fig. 6. The calculated power deposition pattern of the BSD Medical antenna of Fig. 3(b) when placed in a conductive medium of $\sigma = 3$ mho/m instead of the $\sigma = 1.3$ mho/m used in Fig. 3(b). More enhancement of the power deposition near the feed section and less power near the tip are generally observed when comparing this figure with Fig. 3(b).

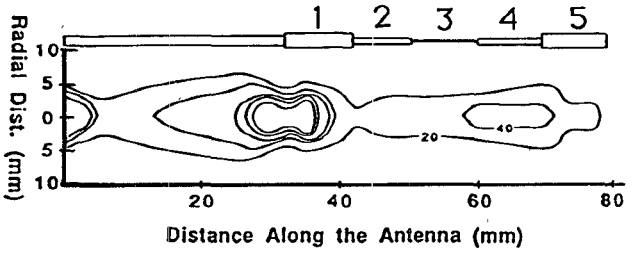

Section No.	1	2	3	4	5
α/β	0.233	0.209	0.139	0.203	0.233

Insulation
3.3 mm O. D., 3.1 mm I.D.
σ =1.3 mho/m

Fig. 7. the calculated power deposition pattern of the BSD Medical antenna of Fig. 3 with the increased diameters of the collars' sections at the feed and the tip. A larger catheter (3.3 mm OD and 3.1 mm ID) was utilized to accommodate the enlarged collars

energy might have been coupled to the last section and the power deposition pattern might have been extended further along the antenna.

Another important observation regarding the capabilities of the numerical model may be illustrated by referring to the BSD antenna shown in Fig. 3. At first, it was not possible to obtain the power deposition pattern with some enhancement near the tip of the antenna (see Fig. 3). In an attempt to understand the discrepancy between the experimental and the numerical results, the tip of the BSD antenna was examined more carefully. It was found that the outer and center conductors were shorted at the tip. Hence, simulating the BSD Medical antenna as an open-ended one similar to all the other designs was incorrect. The power deposition for the case of the short-circuited tip

antenna which was utilized in the BSD design was then computed and the results are shown in Fig. 5. It is clear that the short-circuit termination of the antenna has played an important role in shifting the power deposition pattern and in enhancing it near the tip. This is clearly in excellent agreement with the experimental results shown in Fig. 3.

With confidence in the accuracy of the numerical model, it was then used to examine the effect of varying some of the design parameters and the conductivity of the surrounding medium on the power deposition pattern of these commercial antennas. In this paper we will present results for the BSD antenna, since it represents the most complicated and interesting design. Fig. 6 shows the calculated power deposition pattern of the BSD antenna when placed in a medium of conductivity $\sigma = 3$ mho/m instead of 1.3 mho/m. Comparing the results of Figs. 6 and 3(b) for the two different conductivities clearly shows that an increase in ambient conductivity limits the ability of the middle sections in guiding the energy and hence that the power deposition is enhanced near the center section of the antenna and reduced near the tip. The power deposition pattern of the BSD Medical antenna in a medium of higher conductivity is now similar to that of the uniformly insulated antenna developed by Dartmouth. Another interesting observation was noticed when slight changes in the BSD antenna dimensions were made. Fig. 7 shows the power deposition pattern when the diameters of the two collars were changed from 1.07 to 1.5 mm. It should be noted that in Fig. 7, the dimensions of the catheter were changed so as to accommodate dimensions of the enlarged collars. The change in the diameters of the collars is expected to increase the coupling efficiency, α/β, in these collar sections and hence result in an enhancement in the power deposition near these sections. The results in Fig. 7 show such an enhancement near the feed section and, to a lesser extent, near the tip. The coupling efficiency term, α/β, changed from 0.217 to 0.233, as shown in Figs. 3(b) and 7. Clearly, most of the EM energy was coupled to the ambient near the collar close to the feed section, the matter that limited the availability of the incident energy to the tip section.

IV. Conclusions

The power deposition patterns of several commercially available interstitial antennas were calculated using a new approximated numerical model [2]–[4]. This model calculates the current distribution as well as the near- and far-field radiation characteristics of multisection insulated antennas. The calculation of the current distribution is based on the rigorous theory of insulated antennas developed by King *et al.* [6], while the radiation fields were calculated based on a point-source distribution model. The magnitude and the phase of the point-source distribution are based on the current distribution along the multisection antenna and the radiation efficiency factor, α/β, which is proportional to the radiation losses per wavelength.

Excellent agreement was obtained between the numerical and the experimental power deposition patterns for the Dartmouth D9, the Cheung Hot-Tip, the Cheung two-node, and the BSD antennas [1]. In addition to the numerical confirmation of the measured power deposition patterns of these antennas, the numerical model provides a significant insight into the performance improvement and optimization of these antennas. In particular, we have examined the role of each section, in certain antenna designs, in guiding the EM energy along the antenna versus coupling the energy to the ambient medium. We have also illustrated the effect of changing the diameter of the collars and the conductivity of the ambient medium on this role and hence on the power deposition pattern of these antennas. Other interesting effects such as the tip terminations were examined and their role in changing the antenna pattern was shown. The use of the numerical model to design interstitial antennas of unique capabilities is under way. Utilization of this model to calculate the electromagnetic power deposition pattern in a three-dimensional model of tumors having dielectric properties different from those of the host tissue has also been recently reported [10].

References

[1] T. P. Ryan and J. W. Strohbehn, "A comparison of power deposition for three microwave antennas useds in hyperthermia cancer therapy," in *Proc. 9th Annual Meeting of the Engineering in Medicine and Biology Society* (Boston, MA), Nov. 13–16, 1987.

[2] M. F. Iskander and A. M. Tumeh, "Design optimization of interstitial antennas for microwave hyperthermia," in *IEEE MTT-S Int. Microwave Symp. Dig.* (New York) May 25–27, 1988, pp 151–153.

[3] M. F. Iskander and A. M. Tumeh, "Design optimization of interstitial antennas," *IEEE Trans. Biomed. Eng.*, vol 36, pp. 238–246, Feb. 1989.

[4] A M. Tumeh, "Experimental and numerical study of the optimum design of interstitial antennas for microwave hyperthermia," M S thesis, Electrical Engineering Department, University of Utah, Salt Lake City, 1988.

[5] R. W. P. King, B. S Trembly, and J. W. Strohbehn, "The electromagnetic field of an insulated antenna in a conducting or a dielectric medium," *IEEE Trans. Microwave Theory Tech.*, vol. MTT-31, pp. 574–583, July 1983.

[6] R. W. P. Kind and G. S. Smith, *Antenna in Matter*. Cambridge, MA: MIT Press, 1981.

[7] T. Z Wong, J. W. Strohbehn, K. M. Jones, J. A Mechling, and B. S. Trembly, "SAR patterns from an interstitial microwave antenna-array hyperthermia system," *IEEE Trans. Microwave Theory Tech.*, vol. MTT-34, pp. 560–567, May 1986.

[8] P F. Turner, "Interstitial equal-phased arrays for EM hyperthermia," *IEEE Trans. Microwave Theory Tech*, vol. MTT-34, pp 572–578, May 1986

[9] D J. Lee, M. J O'Neill, K S. Lam, R. Rostock, and W C. Lam, "A new design of microwave interstitial applicators for hyperthermia with improved treatment volume," *Int J Radiat. Oncol Biol Phys.*, vol 12, pp 2003–2008, 1986.

[10] C M Furse and M. F Iskander, "Three-dimensional electromagnetic power deposition in tumors using interstitial arrays," presented at Tenth Annual Meeting of the Bioelectromagnetics Society, Stamford, CT, June 19–23, 1988; also *IEEE Trans. Biomed. Eng*, to be published.

✠

Amer M. Tumeh was born in Amman, Jordan, on August 1, 1962 He received the B.S.E.E and M.S.E.E. degrees from the University of Utah in 1985 and 1988 During the years 1985–1987, his research dealt with

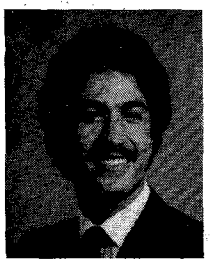

the design and optimization of microwave interstitial antennas for hyperthermia.

In June 1987 he joined the BSD Medical Corporation, where he is currently a member of the Research and Development staff. His research activities have been concerned with developing RF and microwave applicators for hyperthermia cancer treatment.

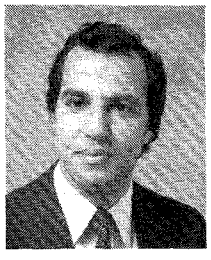

Magdy F. Iskander (S'72–M'76–SM'84) was born in Alexandria, Egypt, on August 6, 1946. He received the B.Sc. degree in electrical engineering from the University of Alexandria, Egypt, in 1969. He received the M.Sc. and Ph.D. degrees in 1972 and 1976, respectively, both in microwaves, from the University of Manitoba, Winnipeg, Manitoba, Canada.

In 1976, he was awarded a National Research Council of Canada Postdoctoral Fellowship at the University of Manitoba. Since 1977 he has been with the Department of Electrical Engineering and the Department of Bioengineering at the University of Utah, Salt Lake City, where he is currently a Professor of Electrical Engineering and a Research Professor of Materials Science and Engineering. In 1981, he received the University of Utah President David P. Gardner Faculty Fellow Award and spent the academic quarter on leave as a Visiting Associate Professor at the Department of Electrical Engineering and Computer Science, Polytechnic Institute of New York, Brooklyn. He spent the summers of 1985 and 1986 at the Chevron Oil Field Research Company, La Habra, CA, as a Visiting Scientist. From September 1986 to May 1987 he spent a sabbatical leave at UCLA, where he worked on the coupling characteristics of microwave integrated circuits to inhomogeneous media, and at the Harvey Mudd College, where he learned about their engineering clinic program. He spent the last four months of the sabbatical leave with the Ecole Superieure d'Electricite, Gif-Sur-Yvette, France, where he worked on microwave imaging. His present fields of interest include the use of numerical techniques in electromagnetics to calculate scattering by dielectric objects, antenna design for medical applications, microwave integrated circuit design, and the use of microwave methods for materials characterization and processing.

Dr. Iskander edited two special issues of the *Journal of Microwave Power*, one on "Electromagnetics and Energy Applications," March 1983, and the other on "Electromagnetic Techniques in Medical Diagnosis and Imaging," September 1983. The holder of seven patents, he has contributed seven chapters to five research books, published more than 80 papers in technical journals, and made more than 150 presentations at technical conferences. In 1983, he received the College of Engineering Outstanding Teaching Award and the College Patent Award for creative, innovative, and practical invention. In 1984, he was selected by the Utah Section of IEEE as the Engineer of the Year. In 1984 he received the Outstanding Paper Award from the International Microwave Power Institute, and in 1985 he received the Curtis W. McGraw ASEE National Research Award for outstanding early achievements by a university faculty member. In 1986 Dr. Iskander established the Engineering Clinic Program in the College of Engineering at the University of Utah. Since then the program has attracted 17 research projects from nine different companies throughout the United States. He is also a member of the IEEE AP-S National Committee on Education and chairman of the subcommittee on the use of computational techniques in electromagnetic education.